

# Optimized Thermoelectric Refrigeration in the Presence of Thermal Boundary Resistance

Anthony M. Pettes, Marc S. Hodes, and Kenneth E. Goodson

**Abstract**—Thermoelectric refrigerators (TEMs) offer several advantages over vapor-compression refrigerators. They are free of moving parts, acoustically silent, reliable, and lightweight. Their low efficiency and peak heat flux capabilities have precluded their use in more widespread applications. Optimization of thermoelectric pellet geometry can help, but past work in this area has neglected the impact of thermal and electrical contact resistances. The present work extends a previous 1-D TEM model to account for a thermal boundary resistance and is appropriate for the common situation where an air-cooled heat sink is attached to a TEM. The model also accounts for the impact of electrical contact resistance at the TEM interconnects. The pellet geometry is optimized with the target of either maximum performance or efficiency for an arbitrary value of thermal boundary resistance for varying values of the temperature difference across the unit, the pellet Seebeck coefficient, and the contact resistances. The model predicts that when the thermal contact conductance is decreased by a factor of ten, the peak heat removal capability is reduced by at least 10%. Furthermore, when the interconnect electrical resistance rises above a factor of ten larger than the pellet electrical resistance, the maximum heat removal capability for a given pellet height is reduced by at least 20% and the maximum coefficient of performance at low  $K_{u-\infty,u}/(NK)$  values is reduced by at least 50%.

**Index Terms**—Contact resistance, superlattices, thermoelectric devices, thermoelectric energy conversion, thermoelectricity.

## NOMENCLATURE

$A_P$	Pellet cross-sectional area [m <sup>2</sup> ].
$A_{\text{sub}}$	Surface area of a TEM substrate [m <sup>2</sup> ].
csi	Controlled-side interface.
$H$	Pellet height [m].
$H_{\text{min}}$	$H$ for which $\Delta T = \Delta T_{\text{max}}$ [m].
$H_0$	$H$ that maximizes $q''_{c,\text{max}}$ [m].
$H_{\text{opt}}$	$H$ for which $\beta = \beta_{\text{max}}$ at given $q''_c$ [m].
$I$	Electrical current [A].
$I_{\text{max}}$	Electrical current at $q''_{c,\text{max}}$ [A].
$I_{\text{opt}}$	Electrical current at $\beta_{\text{max}}$ [A].

Manuscript received November 06, 2007; revised January 18, 2008. First published June 10, 2008; current version published May 28, 2009. This work was supported by Alcatel-Lucent Bell Labs Graduate Research Fellowship Program. This work was recommended for publication by Associate Editor K. Kurabayashi upon evaluation of the reviewers comments.

A. M. Pettes and K. E. Goodson are with the Department of Mechanical Engineering, Stanford University, Stanford, CA 94305 USA (e-mail: apettes@stanford.edu; goodson@stanford.edu).

M. S. Hodes is with the Bell Labs Research Center Ireland, Dublin 15, Ireland (e-mail: hodes@alcatel-lucent.com).

Color versions of one or more of the figures in this paper are available online at <http://ieeexplore.ieee.org>.

Digital Object Identifier 10.1109/TADVP.2008.924221

$k$	Pellet thermal conductivity [W/m · K].
$K$	Thermal conductance of a thermocouple, $2kA_P/H$ [W/K].
$K_{u-\infty,u}$	usi-to-ambient thermal conductance [W/K].
$K''_{u-\infty,u}$	$K_{u-\infty,u}/A_{\text{sub}}$ [W/m <sup>2</sup> · K].
$N$	Number of thermocouples in a TEM, $A_{\text{sub}}\phi/(2A_P)$ .
$q''$	Heat flux [W/m <sup>2</sup> ].
$q''_{c,\text{max}}$	$q''_c$ maximized with respect to $I$ [W/m <sup>2</sup> ].
$q''_{c,\text{peak}}$	$q''_c$ maximized with respect to $I$ and $H$ [W/m <sup>2</sup> ].
$R$	Ohmic resistance of a thermocouple, $2\rho H/A_P$ [ $\Omega$ ].
$R_{ec-\rho}$	Electrical contact resistivity [ $\Omega\text{m}^2$ ].
$R_{ec-R}$	Electrical contact resistance of a thermocouple, $4R_{ec-\rho}/A_P$ [ $\Omega$ ].
$T$	Temperature [K].
usi	Uncontrolled-side interface.
$V_0$	Voltage in lead connected to n-type pellet [V].
$V_N$	Voltage in lead connected to p-type pellet [V].
$V''_{\text{TEM}}$	Voltage difference across TEM per unit substrate area of TEM [V/m <sup>2</sup> ].
$\dot{W}''_{\text{TEM}}$	Rate of electrical work done on TEM per unit substrate area [W/m <sup>2</sup> ].

## Greek Symbols

$\alpha$	Seebeck coefficient [V/K].
$\alpha_{p,n}$	$\alpha_p - \alpha_n$ [V/K].
$\beta$	Coefficient of performance of a refrigerator.
$\beta_{\text{max}}$	$\beta$ maximized with respect to $I$ for given $H$ .
$\Delta T_{\text{max}}$	Maximum $\Delta T$ for which $q''_c = 0$ [K].
$\rho$	Pellet electrical resistivity [ $\Omega\text{m}$ ].
$\phi$	Pellet packing density, $2NA_P/A_{\text{sub}}$ .

## Subscripts

$\infty$	Ambient.
$c$	Controlled-side interface.
$cp$	Controlled point.
$n$	$n$ -type pellet.
$p$	$p$ -type pellet.
$u$	Uncontrolled-side interface.

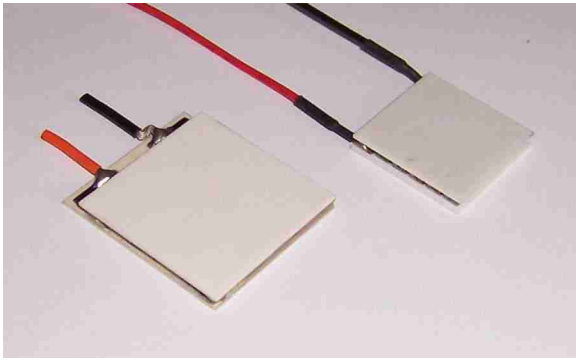


Fig. 1. Single-stage bulk thermoelectric modules. Dimensions of the left and right TEMs are 3.4 cm  $\times$  3.0 cm  $\times$  3.6 mm and 2.3 cm  $\times$  2.3 cm  $\times$  3.6 mm, respectively.

## I. INTRODUCTION

**S**OLID-STATE thermoelectric modules (TEMs) use electron transport to cool, heat or generate electric power in accordance with design specifications (Fig. 1). TEMs are versatile devices with applications ranging from electronics cooling to precision temperature control of photonic components to power generation from waste heat. They are free of moving parts, acoustically and mechanically silent, reliable, and lightweight. Thermoelectric refrigerators offer limited heat flux capacity and low thermodynamic efficiency when compared with vapor compression refrigerators. As a result of these limitations, developing means to increase TEM performance and efficiency is an important task. Since the improvements of thermoelectric materials in the 1950s [1], several approaches have been taken to optimize thermoelectric devices. Thermoelectric materials with better combinations of properties, such as the low-dimensional materials proposed by Dresselhaus *et al.* and Venkatasubramanian *et al.*, have increased thermoelectric figure of merit [2], [3]. Advances in the packaging of thermoelectric devices can improve both heat flux capacity and efficiency. For example, reduction in the electrical and/or thermal contact resistances at the interconnects, which are significant sources of irreversibility, can be of major benefit. Finally, improved system-level designs are known to increase performance or efficiency of TEMs. For example, judicious selection of the heat sink's thermal resistance can significantly reduce the maximum power consumption of a TEM requiring switching between heating mode, where a poor heat sink is desirable, and cooling mode, where an efficient heat sink is beneficial [4]. These advances have given rise to opportunities for geometric design optimization in order to fully harvest the benefits of new materials, which are currently absorbed by significant irreversibility losses due to thermal and electrical boundary resistances.

### A. Motivation

Fifty years after Ioffe's renovation of thermoelectric materials, designers are still lacking a cogent, generalized analysis in which a given set of geometric constraints along with material data may be manipulated in order to fine tune system-level parameters such as the cooling flux, coefficient of performance, and operating current and voltage per unit footprint of a TEM.

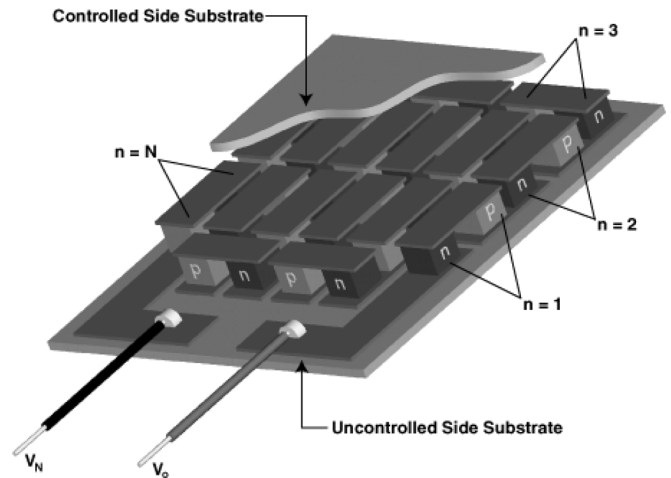


Fig. 2. Cutaway view of a TEM.

This work provides designers with a procedure to calculate the optimum pellet height to maximize performance or efficiency at a specified performance given the relevant operational parameters, i.e., control point temperature, ambient temperature, and thermal resistance of the heat sink. Moreover, designers are provided a means to calculate pellet area to best match TEM voltage demands to those from available power sources.

The essence of this study lies in the advancement of previous work through the inclusion of thermal boundary resistance at the uncontrolled side interface. This is accomplished by generalizing the analysis of Hodes [5] by prescribing a mixed boundary condition at the uncontrolled side interface (Fig. 3). Accordingly, thermal resistances (including constriction/spreading resistances) between the user and its local ambient are embedded in  $R_{u-\infty,u}$ . The results are placed in context in Section III for representative operating conditions in a conventional bismuth telluride ( $\text{Bi}_2\text{Te}_3$ ) TEM coupled to a representative heat sink.

### B. Conventions

A single-stage TEM is shown in Fig. 2 following the nomenclature of Hodes [6]. It consists of an array of *p*-type and *n*-type pellets connected electrically in series and thermally in parallel between ceramic substrates. Each adjacent pair of *p*-type and *n*-type pellets is referred to as a thermocouple and there are *N* thermocouples in a TEM. Here it is assumed that the controlled side of a TEM is that which does not connect to the external leads according to Fig. 2. The other side is defined as the uncontrolled side.<sup>1</sup> The csi and usi are defined as the interfaces between the pellets and the controlled and uncontrolled sides, respectively (Fig. 3).

The temperatures at the csi and the usi are denoted by  $T_c$  and  $T_u$ , respectively. Thermodynamically, a TEM operates in refrigeration mode when there is heat transfer from the controlled-side substrate into the csi (Fig. 4) and, moreover, the temperature of the csi is below that of the usi [6]. An infinite thermal conductance approximation is made between the csi and

<sup>1</sup>Prior investigations have defined hot and cold sides of TEMs in their analyses, resulting in analytical complications since either side may be hot or cold relative to the opposite side in precision temperature control applications.

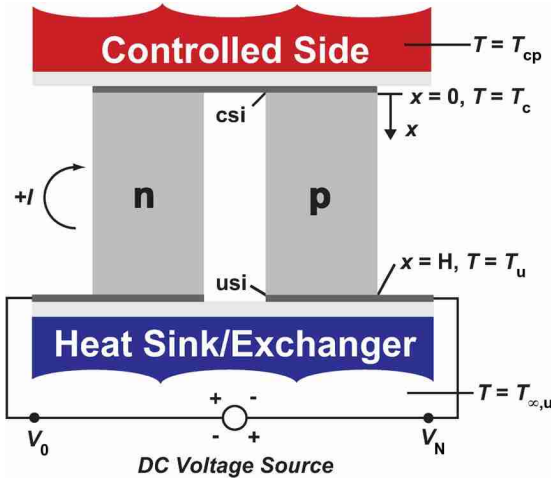


Fig. 3. Schematic representation of a single-thermocouple TEM operating in refrigeration mode.

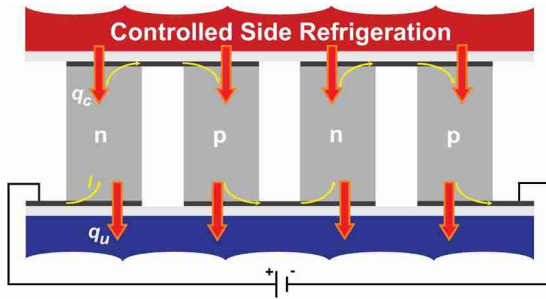


Fig. 4. Cross-sectional view of a TEM depicting Peltier-induced refrigeration of the controlled side. Note that thermoelectric pellets are connected electrically in series and thermally in parallel.

the component mounted to a TEM such that  $T_{cp} = T_c$ . The uncontrolled side temperature  $T_u$  is subjected to the ambient temperature  $T_{\infty,u}$  through a usi-to-ambient thermal boundary conductance  $K_{u-\infty,u}$ . Currents are taken to be positive when positive charge carriers flow from  $n$ -type pellets to  $p$ -type pellets at the controlled side of a TEM, as shown in Fig. 3. Since Seebeck coefficients  $\alpha_p$  and  $\alpha_n$  are positive and negative quantities, respectively, heat is reversibly absorbed at the csi and reversibly released at the usi by the Peltier effect when current is positive.

## II. THERMOELECTRIC PELLET DESIGN

### A. Negligible Electrical Contact Resistance

Equations governing TEM operation have been developed in detail by Ioffe [1], Kraus and Bar-Cohen [7], Yamanashi [8], and Semenyuk [9], among others. In this study, the equations for a thermoelectric module are introduced on a flux basis under a 1-D, steady state model assuming isotropic and temperature-independent material properties with boundary conditions of the first kind at the csi and of the third kind at the usi. Surface energy balances at the csi and usi yield the respective heat fluxes as a function of current, material geometry and properties, controlled side temperature, ambient temperature, and thermal boundary conductance

$$q_c'' = \phi \left[ \frac{I\alpha_{p,n}T_c}{2A_P} - \frac{k(T_u - T_c)}{H} - \frac{I^2\rho H}{2A_P^2} \right] \quad (1)$$

$$K_{u-\infty,u}''(T_u - T_{\infty,u}) = \phi \left[ \frac{I\alpha_{p,n}T_u}{2A_P} - \frac{k(T_u - T_c)}{H} + \frac{I^2\rho H}{2A_P^2} \right] \quad (2)$$

where  $\phi$  is the pellet packing density. Similarly, the per-unit-footprint rate of electrical work done on a TEM and the per-unit-footprint voltage difference across a TEM while current flows through it are

$$\dot{W}_{\text{TEM}}'' = q_u'' - q_c'' = \phi I \left[ \frac{\alpha_{p,n}(T_u - T_c)}{2A_P} + \frac{I\rho H}{A_P^2} \right] \quad (3)$$

$$V_{\text{TEM}}'' = \frac{V_0 - V_N}{A_{\text{sub}}} = \phi \left[ \frac{\alpha_{p,n}(T_u - T_c)}{2A_P} + \frac{I\rho H}{A_P^2} \right] \quad (4)$$

$\dot{W}_{\text{TEM}}''$  will always be positive since work is done on a TEM by a dc power supply when it is operating in refrigeration mode.

Solving (2) yields  $T_u$  as a function of the known temperature  $T_{\infty,u}$ . Substituting  $T_u$  into (1) yields  $q_c''$  as a function of known temperatures  $T_c$  and  $T_{\infty,u}$

$$q_c'' = \underbrace{-\frac{\phi\rho H}{2A_P^2}}_{c_1} I^2 + \underbrace{\frac{\phi\alpha_{p,n}T_c}{2A_P}}_{c_2} I + \underbrace{\frac{\phi k T_c}{H}}_{c_7} - \frac{\underbrace{\frac{\phi^2\rho k}{2A_P^2}}_{c_3} I^2 + \underbrace{\frac{\phi^2 k^2 T_c^2}{H}}_{c_4} + \underbrace{\frac{\phi k K_{u-\infty,u}'' T_{\infty,u}}{H}}_{c_5}}{\underbrace{-\frac{\phi\alpha_{p,n}}{2A_P}}_{c_5} I + \underbrace{K_{u-\infty,u}'' + \frac{\phi k}{H}}_{c_6}} \quad (5)$$

Differentiating (5) with respect to  $I$ , setting the result equal to zero, and solving for the single real root of (6) yields the current  $I_{\text{max}}$  for which  $q_c''$  is maximized

$$I_{\text{max}}^3 + a_2 I_{\text{max}}^2 + a_1 I_{\text{max}} + a_0 = 0 \quad (6)$$

where  $a_2 = (4c_1c_5c_6 + c_2c_5^2 - c_3c_5)/(2c_1c_5^2)$ ,  $a_1 = (c_1c_6^2 + c_2c_5c_6 - c_3c_6)/(c_1c_5^2)$ ,  $a_0 = (c_2c_6^2 + c_4c_5)/(2c_1c_5^2)$ , and constants  $c_i$  are as shown in (5). The corresponding heat flux at the csi  $q_{c,\text{max}}''$  for a given pellet height is obtained by substituting  $I_{\text{max}}$  into (5)

$$q_{c,\text{max}}''(H) = \underbrace{-\frac{\phi\rho I_{\text{max}}(H)^2}{2A_P^2}}_{d_1} H + \underbrace{\frac{\phi k T_c}{H}}_{d_2} H^{-1} - \frac{\underbrace{\frac{\phi^2 k^2 T_c}{H}}_{d_3} H^{-2} + \underbrace{\frac{\phi k K_{u-\infty,u}'' T_{\infty,u}}{H}}_{d_4} H^{-1} + \underbrace{\frac{\phi^2 \rho k I_{\text{max}}(H)^2}{2A_P^2}}_{d_5}}{\underbrace{\frac{\phi k}{H}}_{d_6} H^{-1} + \underbrace{K_{u-\infty,u}'' - \frac{\phi\alpha_{p,n} I_{\text{max}}(H)}{2A_P}}_{d_7}} + \underbrace{\frac{\phi\alpha_{p,n} T_c I_{\text{max}}(H)}{2A_P}}_{d_8} \quad (7)$$

The pellet height  $H_0$  corresponding to the peak heat flux at the csi  $q_{c,\text{peak}}''$  is determined by numerically differentiating (7) with

respect to  $H$ . The peak heat flux  $q''_{c,peak}$  is then obtained by substituting  $H_0$  into (7).

The coefficient of performance  $\beta$  of a TEM operating in refrigeration mode ( $q''_c > 0$ ) is defined as the rate of cooling provided by a TEM divided by the rate of work done on a TEM

$$\beta = \frac{q''_c}{\dot{W}''_{TEM}} \quad (8)$$

Differentiating (8) with respect to  $I$ , setting the result equal to zero, and solving for the appropriate real root of (9) yields the current  $I_{opt}$  for which  $\beta$  is maximized

$$I_{opt}^4 + f_3 I_{opt}^3 + f_2 I_{opt}^2 + f_1 I_{opt} + f_0 = 0 \quad (9)$$

where  $f_3 = 4\alpha_{p,n}T_{\infty,u}/R$ ,  $f_2 = 2K(3T_c - 5T_{\infty,u}) - 2K_{u-\infty,u}(T_c + T_{\infty,u})/(NR) - 4\alpha_{p,n}^2 T_c T_{\infty,u}/R^2$ ,  $f_1 = -8K(T_c - T_{\infty,u})(\alpha_{p,n}^2 NT_c + RK_{u-\infty,u} + NK R)/(\alpha_{p,n} NR^2)$ , and  $f_0 = 4KK_{u-\infty,u}(T_c - T_{\infty,u})^2/(NR^2)$ . The maximum possible coefficient of performance  $\beta_{max}$  for a given pellet height is obtained by substituting  $I_{opt}$  into (8).

In the absence of electrical contact resistance, the maximum temperature difference across a TEM that will accommodate refrigeration ( $\Delta T_{max} = T_u(I_{max}) - T_c$ ) occurs when  $q''_{c,max} = 0$ . Substituting  $I = I_{max}$  into (1) and setting (1) equal to zero yields  $\Delta T_{max}$  as a function of  $H$

$$\Delta T_{max}(H) = \frac{H}{k} \left( \frac{I_{max}(H)}{A_P} \right) \left[ \frac{\alpha_{p,n} T_c}{2} - \frac{\rho H}{2} \left( \frac{I_{max}(H)}{A_P} \right) \right] \quad (10)$$

### B. Finite Electrical Contact Resistance

The assumption of negligible contact resistance in Section II-A is relaxed by modifying the surface energy balances at the csi and usi to include an additional generation term to account for interfacial Ohmic heating. Consequentially, electrical resistivity  $\rho$  becomes a function of pellet height and is replaced with an effective resistivity  $\rho_{eff}$  in order to account for contributions from both bulk and interfacial Ohmic resistances

$$\rho_{eff} = \rho + \frac{2R_{ec-\rho}}{H} \quad (11)$$

where  $R_{ec-R}$  is the electrical contact resistance of a thermocouple ( $R_{ec-R} = 4R_{ec-\rho}/A_P$ ) and  $R_{ec-\rho}$  is the electrical contact resistivity of an electrical interconnect. As a result of the inclusion of finite electrical contact resistance, the surface energy balances at the csi (1) and usi (2) are recast as follows:

$$q''_c = \phi \left[ \frac{I\alpha_{p,n}T_c}{2A_P} - \frac{k(T_u - T_c)}{H} - \frac{I^2\rho_{eff}H}{2A_P^2} \right] \quad (12)$$

$$\begin{aligned} q''_u &= K''_{u-\infty,u}(T_u - T_{\infty,u}) \\ &= \phi \left[ \frac{I\alpha_{p,n}T_u}{2A_P} - \frac{k(T_u - T_c)}{H} + \frac{I^2\rho_{eff}H}{2A_P^2} \right]. \end{aligned} \quad (13)$$

Due to the additional dependence of  $q''_c$  on  $H$ , (3)–(10) are no longer valid and are instead solved numerically.

### C. Numerical Methods

The coupled equations developed above were solved numerically using a discretization scheme compatible with logarithmic scaling for variables  $I$ ,  $H$ ,  $K''_{u-\infty,u}$ , and  $R_{ec-\rho}$ . This discretization scheme enhanced resolution at low values of  $I$ ,  $H$ ,  $K''_{u-\infty,u}$ , and  $R_{ec-\rho}$  while significantly reducing computing costs as compared to a traditional linear discretization. Mesh independence was obtained for 20 data points in each  $10^{i+1} - 10^i$  segment of the logarithmic scale. The roots of the monic polynomials given in (6) and (9) were solved numerically by computing the eigenvalues of their respective companion matrices, and verified by comparison to the limiting cases of this model.

### D. Nondimensionalization

The relative importance of thermal boundary and electrical contact resistance in TEM design are revealed through nondimensionalization of conductance and resistance ratios. The first nondimensional group of interest  $HK''_{u-\infty,u}/(\phi k)$  is the ratio of the boundary to pellet thermal conductance, while the second nondimensional group of interest  $2R_{ec-\rho}/(H\rho)$  is the ratio of the interconnect to pellet electrical resistance

$$\frac{K_{u-\infty,u}}{NK} = \frac{HK''_{u-\infty,u}}{\phi k} \quad (14)$$

$$\frac{R_{ec-R}}{R} = \frac{2R_{ec-\rho}}{\rho H} \quad (15)$$

Nondimensionalization of (1)–(13) in accordance with the Buckingham  $\pi$  theorem [10], however, is beyond the scope of this analysis.

## III. ILLUSTRATIVE RESULTS

The properties of conventional bismuth telluride pellets operating near room temperature ( $\alpha_{p,n} = 4 \times 10^{-4}$  V/K,  $k = 1.5$  W/m·K,  $\rho = 1 \times 10^{-5}$   $\Omega \cdot m$ ) are used to illustrate the application of the foregoing analysis [11]. The cross-sectional pellet area  $A_P$  and cross-sectional substrate area  $A_{sub}$  are anchored at  $1.4^2$  mm<sup>2</sup> and  $8A_P$ , respectively, while the pellet packing density  $\phi$  is 0.5 and the number of thermocouples  $N$  is 2. The controlled-side interface temperature is set to 290 K and the uncontrolled-side temperature is set to 310 K unless otherwise stated. The pellet packing density is set to 0.5 for a four-pellet TEM with  $A_P = 1.4^2$  mm<sup>2</sup>,  $A_{sub} = 8A_P$ , and  $N = 2$ . Typical thermal boundary resistances at the uncontrolled-side interface in modern devices range from 200 to 50 000 W/m<sup>2</sup> · K [12], [13]. Typical electrical contact resistivities in modern thermoelectric devices range from  $5 \times 10^{-9}$   $\Omega \cdot m^2$  to  $5 \times 10^{-11}$   $\Omega \cdot m^2$  [14], [15].

### A. Negligible Electrical Contact Resistance

Heat flux, coefficient of performance, and voltage across a TEM per unit footprint are plotted versus current for selected values of cross-sectional pellet area in Fig. 5. A key result is that maximum performance  $q''_{c,max}$  and maximum coefficient of performance  $\beta_{max}$  are independent of pellet cross-sectional area  $A_P$ . The coefficient of performance for any arbitrary cooling

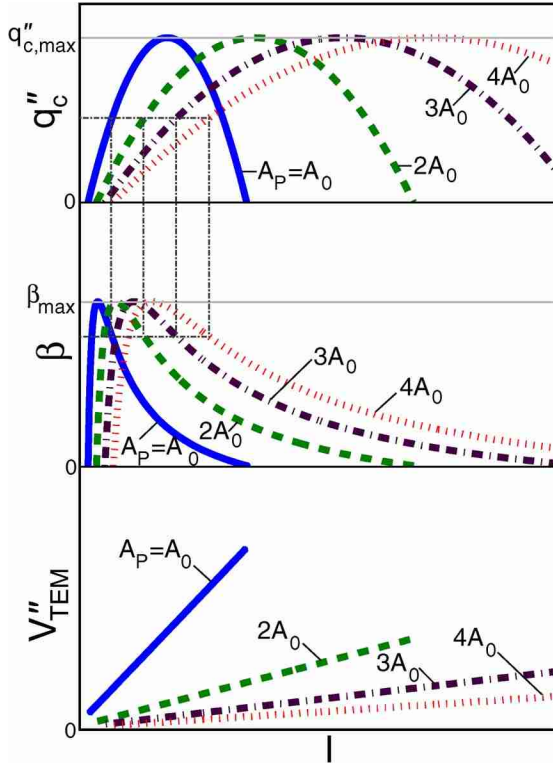


Fig. 5. Dependence of cooling flux, coefficient of performance, and voltage per unit area on current for a given pellet height in the absence of electrical contact resistance, showing the independence of pellet cross-sectional area on maximum performance and efficiency and the dependence of pellet cross-sectional area on operating voltage and current.

flux is also independent of  $A_P$ . The operating voltage and current, however, are dependent on  $A_P$ , which may be tuned to closely match available voltages to reduce or eliminate ac-dc power conversion losses.

Heat flux, coefficient of performance, and voltage across a TEM per unit footprint are plotted versus current for selected values of pellet height in Fig. 6, illustrating the dependence of maximum efficiency  $\beta_{\max}$  on pellet height  $H$ . It is evident that the coefficient of performance for any arbitrary cooling flux is dependent on  $H$  and, as  $H \rightarrow \infty$ , the maximum efficiency approaches the limiting case of zero thermal boundary resistance as Ohmic pellet resistance becomes the dominant form of irreversibility. It is also evident that there exists an optimum pellet height  $H_0$  for which  $q_{c,\max}''$  is maximized. Furthermore, the addition of thermal boundary resistance results in irreversibility losses that force a dependence of  $\beta_{\max}$  on  $H$  similar to the dependence caused by irreversibility losses due solely to electrical contact resistance in the previous isothermal model [5].

The maximum temperature difference across a TEM operating in refrigeration mode as a function of  $HK_{u-\infty,u}''/(\phi k)$  (a measure of conductance per unit area of the heat sink to bulk conductance of the pellets) is shown in Fig. 7. In this figure,  $\phi = 0.5$ ,  $K_{u-\infty,u}'' = 795 \text{ W/m}^2 \cdot \text{K}$ ,  $k_{\text{pellet}} = 1.5 \text{ W/m} \cdot \text{K}$ ,  $k = 0.5, 1.0, 2.0, 3.0 \times k_{\text{pellet}}$ , and  $10 \mu\text{m} \leq H \leq 10 \text{ mm}$ . It is evident that as  $HK_{u-\infty,u}''/(\phi k) \rightarrow \infty$ ,  $\Delta T_{\max} \rightarrow \alpha_{p,n}^2 T_c^2 / (8k\rho)$ , its value for the limiting case of the isothermal boundary condition model [5]. The increasing dependence on pellet height for decreasing values of  $HK_{u-\infty,u}''/(\phi k)$  signifies that  $\Delta T_{\max}$

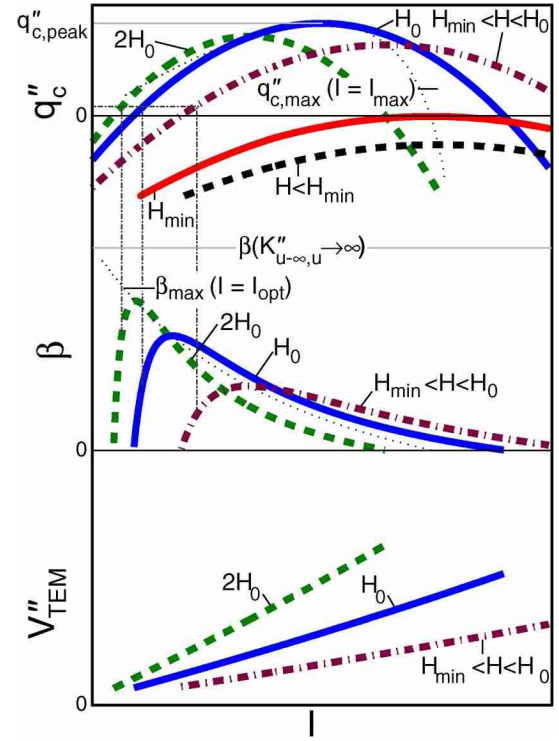


Fig. 6. Dependence of cooling flux, coefficient of performance, and voltage per unit area on current for a given pellet cross-sectional area in the absence of electrical contact resistance, showing the importance of pellet height on design considerations.

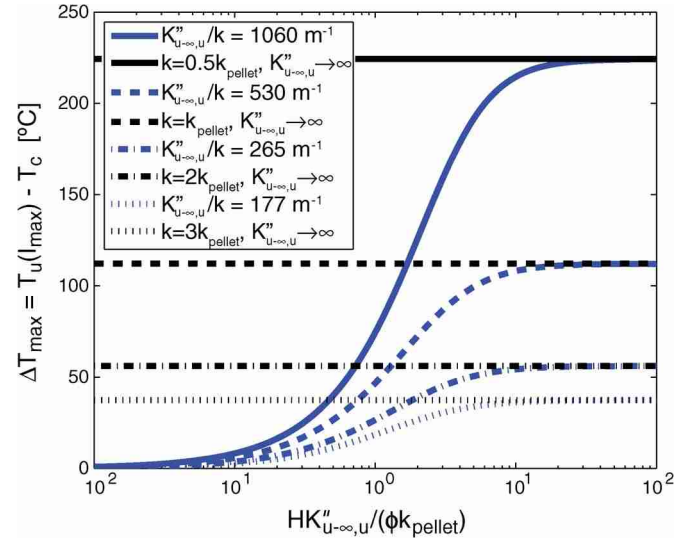


Fig. 7. Competing influences of boundary and pellet thermal conductances on the maximum possible temperature difference across a TEM operating in refrigeration mode in the absence of electrical contact resistance. The limiting case as  $K_{u-\infty,u}'' \rightarrow \infty$  is given by  $\Delta T_{\max} = \alpha_{p,n}^2 T_c^2 / (8k\rho)$ .

is optimized for larger pellet heights and heat sink conductance values coupled with poor thermal conductivity of the pellet that effectually mitigates the influence of  $T_u$  on  $T_c$ . It is also shown that  $\Delta T_{\max}$  increases for lower values of pellet thermal conductivity, an argument for thermoelectric materials with low thermal conductivity and high electrical conductivity such as the recent findings by Chiritescu *et al.* [16].

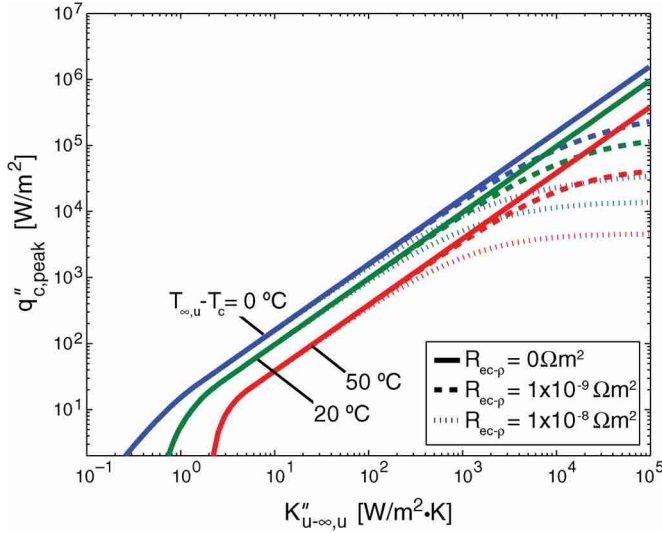


Fig. 8. Competing influences of thermal boundary conductance, interconnect electrical resistance, and csi-to-ambient temperature difference on peak cooling flux.

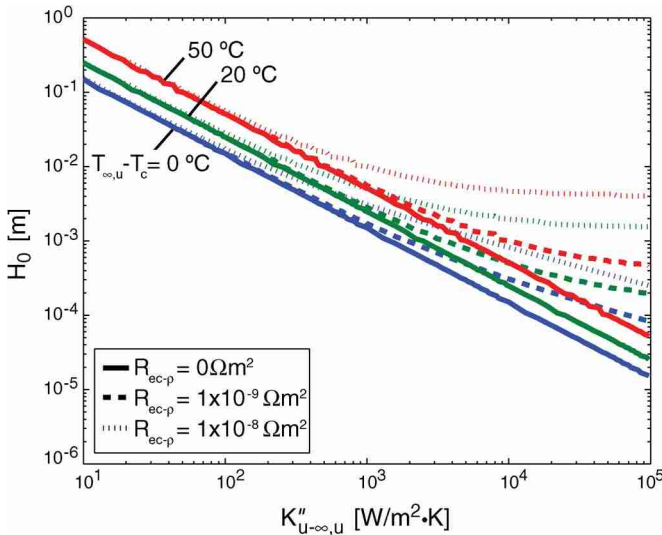


Fig. 9. Competing influences of thermal boundary conductance, interconnect electrical resistance, and csi-to-ambient temperature difference on pellet height corresponding to peak cooling flux shown in Fig. 8.

### B. Finite Electrical Contact Resistance

Peak performance and corresponding pellet height as a function of  $K''_{u-\infty,u}$ ,  $R_{ec-p}$ , and  $\Delta T = T_{\infty,u} - T_c$  are shown in Figs. 8 and 9, respectively. Due to the introduction of additional reversibility, peak performance is degraded by increases in  $R_{ec-p}$  and  $\Delta T$  as well as for decreases in  $K''_{u-\infty,u}$ . Similarly, the pellet height corresponding to peak performance is increased by increases in  $R_{ec-p}$  and  $\Delta T$  as well as for decreases in  $K''_{u-\infty,u}$ . It is also evident that electrical contact resistance becomes the dominant limiting factor of  $q''_{c,peak}$  when the thermal boundary conductance is above  $\sim 10^2 \text{ W/m}^2 \cdot \text{K}$ . Figs. 8 and 9 are helpful in illustrating when the focus of TEM design should shift from improving  $K''_{u-\infty,u}$  to improving  $R_{ec-p}$ , and *vice versa*.

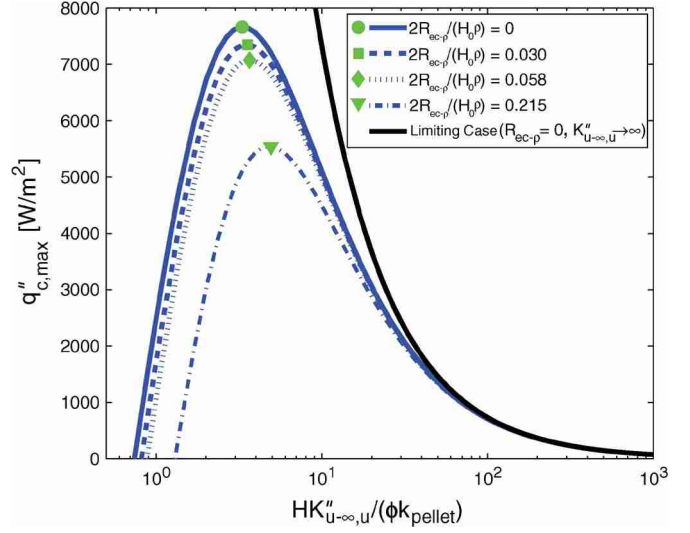


Fig. 10. Dependence of maximum cooling flux on thermal and electrical resistances, showing the importance of boundary to pellet resistance ratios on design considerations.

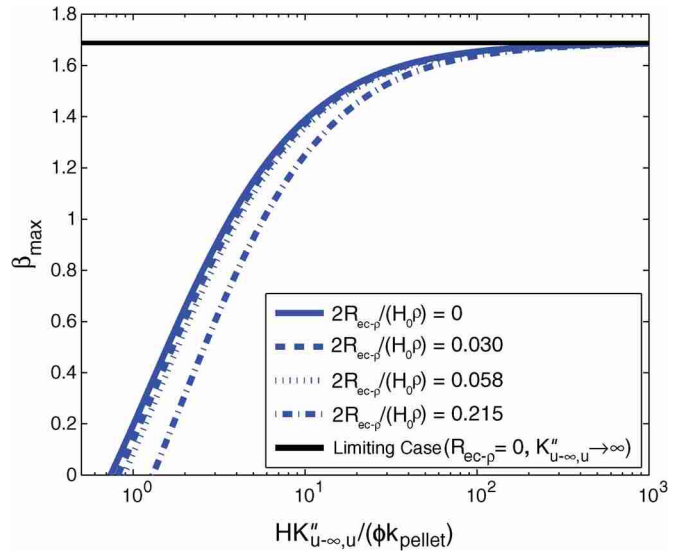


Fig. 11. Dependence of maximum coefficient of performance on thermal and electrical resistances, showing the importance of boundary to pellet resistance ratios on design considerations.

Maximum performance and efficiency as a function of  $HK''_{u-\infty,u}/(\phi k)$  and  $2R_{ec-p}/(H\rho)$  are shown in Figs. 10 and 11, respectively. In this figure,  $\phi = 0.5$ ,  $K''_{u-\infty,u} = 795 \text{ W/m}^2 \cdot \text{K}$ ,  $k = 1.5 \text{ W/m} \cdot \text{K}$ ,  $\rho = 1 \times 10^{-5} \Omega \text{m}$ ,  $R_{ec-p} = 0, 5 \times 10^{-10}, 1 \times 10^{-9}, 5 \times 10^{-9} \Omega \text{m}^2$ , and  $1 \mu\text{m} \leq H \leq 1 \text{ m}$ . As the ratio of interconnect to pellet electrical resistance increases, the peak cooling flux decreases, its corresponding pellet height increases, and the maximum efficiency decreases, especially for low values of the boundary to pellet thermal conductance ratio.

Fig. 12 displays the maximum temperature difference across a TEM operating in refrigeration mode as a function of  $HK''_{u-\infty,u}/(\phi k)$  and  $2R_{ec-p}/(H\rho)$ . In this figure,  $\phi = 0.5$ ,  $K''_{u-\infty,u} = 795 \text{ W/m}^2 \cdot \text{K}$ ,  $k_{\text{pellet}} = 1.5 \text{ W/m} \cdot \text{K}$ ,  $\rho = 1 \times 10^{-5} \Omega \cdot \text{m}$ ,  $R_{ec-p} = 0, 5 \times 10^{-10}, 1 \times 10^{-9}$ ,

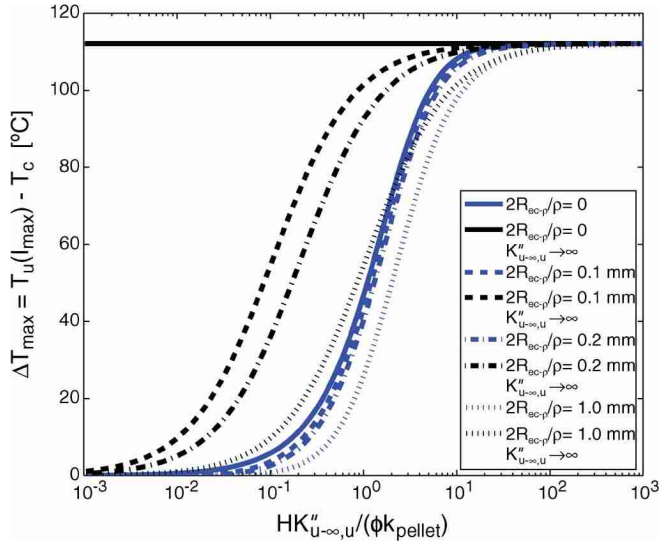


Fig. 12. Competing influences of thermal and electrical resistances on the maximum temperature difference across a TEM operating in refrigeration mode. The limiting case as  $R_{ec-\rho} \rightarrow \infty$  and  $K''_{u-\infty,u} \rightarrow \infty$  is given by  $\Delta T_{\max} = \alpha_{p,n}^2 T_c^2 / (8k\rho + 16kR_{ec-\rho}/H)$ .

$5 \times 10^{-9} \Omega \cdot \text{m}^2$ , and  $1 \mu\text{m} \leq H \leq 1 \text{ m}$ . The increasing dependence on pellet height for decreasing values of  $HK''_{u-\infty,u}/(\phi k)$  signifies that  $\Delta T_{\max}$  is optimized for larger pellet heights and heat sink conductances coupled with poor pellet thermal conductivity that mitigates the influence of  $T_u$  on  $T_c$ . Accordingly, the introduction of electrical contact resistance adds further irreversibility into the system and requires a larger pellet height to achieve an equivalent  $\Delta T_{\max}$ . As  $HK''_{u-\infty,u}/(\phi k)$  approaches  $\infty$ ,  $\Delta T_{\max}$  approaches  $\alpha_{p,n}^2 T_c^2 / (8k\rho + 16kR_{ec-\rho}/H)$ , its value for the limiting case of the isothermal boundary condition model [5].

#### IV. CONCLUSION

A procedure for calculating the optimum pellet height to maximize performance or efficiency at a specified performance given the control point temperature, ambient temperature, and thermal resistance of the heat sink has been provided. The inclusion of finite thermal and electrical boundary resistances leads the coefficient of performance  $\beta$  for a given cooling flux to be determined by the pellet height  $H$  and operating current  $I$ . While  $\beta$  is significantly influenced by  $H$ , it is unaffected by the pellet cross-sectional area  $A_P$ . For a given  $K''_{u-\infty,u}$ ,  $R_{ec-\rho}$ , and  $q_c'' < q_{c,\text{peak}}''$ , for example, there is an  $H$  such that  $\beta = \beta_{\max}$ . Once  $H$  has been determined to maximize  $\beta$  for a given heat flux below the peak heat flux,  $A_P$  can be designed to best satisfy packaging and power requirements. If operating at  $q_{c,\text{peak}}''$ , however, the TEM will be constrained to a single pellet height  $H_0$  and coefficient of performance  $\beta(q_{c,\text{peak}}'')$ .

The existence of a transition point when TEM designers should shift their focus from improving  $K''_{u-\infty,u}$  to improving  $R_{ec-\rho}$ , and *vice versa*, has been presented. For given values of  $\Delta T$  and  $R_{ec-\rho}$ , Figs. 8 and 9 elucidate the relative worth of increasing  $K''_{u-\infty,u}$  before Ohmic heating and Fourier conduction through finite temperature gradients begin to dominate entropy generation effects. The model predicts, for example,

that when the thermal contact conductance is decreased by a factor of ten, the peak heat removal capability is reduced by at least 10%. Furthermore, when the interconnect electrical resistance rises above a factor of ten larger than the pellet electrical resistance, the maximum heat removal capability for a given pellet height is reduced by at least 20% and the maximum coefficient of performance at low  $HK''_{u-\infty,u}/(\phi k)$  values is reduced by at least 50%.

In combination with advances in material properties of thermoelectrics, the design enhancements brought forth through this work will allow designers to recast thermoelectric devices as viable competitors in a field driven by performance and thermodynamic efficiency. Potential applications of results include the combination of this work with variable conductance heat sink research to reduce the power consumption of novel precision temperature control solutions [17]. This work may also serve as a precursor to the investigation of interfacial electron/phonon phenomena since interfacial resistance plays an increasingly significant role as the pellet height approaches the microscale regime [18].

#### REFERENCES

- [1] A. F. Ioffe, *Semiconductor Thermoelements and Thermoelectric Cooling* Transl. Russian. London, U.K.: Infosearch, 1957.
- [2] L. D. Hicks and M. S. Dresselhaus, "Effect of quantum-well structures on the thermoelectric figure of merit," *Phys. Rev. B*, vol. 47, no. 19, pp. 12727–12731, May 1993.
- [3] R. Venkatasubramanian, E. Siivola, T. Colpitts, and B. O'Quinn, "Thin-film thermoelectric devices with high room-temperature figures of merit," *Nature*, vol. 413, pp. 597–602, Oct. 2001.
- [4] M. Hodes, "Precision temperature control of an optical router," in *Handbook of Heat Transfer Calculations*. New York: McGraw-Hill, 2006.
- [5] M. Hodes, "Optimal pellet geometries for thermoelectric refrigeration," *IEEE Tran. Compon. Packag. Technol.*, vol. 30, no. 1, pp. 50–58, Mar. 2007.
- [6] M. Hodes, "On one-dimensional analysis of thermoelectric modules (TEMs)," *IEEE Trans. Compon. Packag. Technol.*, vol. 28, no. 2, pp. 218–229, Jun. 2005.
- [7] A. D. Kraus and A. Bar-Cohen, *Thermal Analysis and Control of Electronic Equipment*. New York: McGraw-Hill, 1983.
- [8] M. Yamanashi, "A new approach to optimum design in thermoelectric cooling systems," *J. Appl. Phys.*, vol. 80, no. 9, pp. 5494–5502, 1996.
- [9] V. A. Semenyuk, "Thermoelectric cooling of electro-optic components," in *Thermoelectrics Handbook: Macro to Nano*, D. M. Rowe, Ed. Boca Raton, FL: CRC Press, 2006, ch. 58, pp. 58-1–58-21.
- [10] E. Buckingham, "On physically similar systems; illustrations of the use of dimensional equations," *Phys. Rev.*, vol. 4, no. 4, pp. 345–376, Oct. 1914.
- [11] "Melcor Thermal Solutions," Melcor Corp., Trenton, NJ, 2002.
- [12] D. B. Tuckerman and R. F. W. Pease, "High-performance heat sinking for VLSI," *IEEE Electron Device Lett.*, vol. 2, no. 5, pp. 126–129, May 1981.
- [13] F. P. Incropera and D. P. DeWitt, *Fundamentals of Heat and Mass Transfer*, 5th ed. New York: Wiley, 2002.
- [14] V. P. Plekhotkin, M. F. Tkachenko, T. M. Melikhova, and L. A. Bondarevskaya, "Determination of the optimal depth of thermoelectric battery cells taking into account the effects of electrical contacts," *Geliotekhnika*, vol. 3, pp. 35–37, 1981.
- [15] H. Bottner, J. Nurnus, A. Gavrikov, G. Kuhner, M. Jagle, C. Kunzel, D. Eberhard, G. Plescher, A. Schubert, and K. Schlereth, "New thermoelectric components using microsystem technologies," *J. Microelectromechan. Syst.*, vol. 13, no. 3, pp. 414–420, Jun. 2004.
- [16] C. Chiritescu, D. G. Cahill, N. Nguyen, D. Johnson, A. Bodapati, P. Kellinski, and P. Zschack, "Ultralow thermal conductivity in disordered, layered  $\text{WSe}_2$  crystals," *Science*, vol. 315, pp. 351–353, Jan. 2007.
- [17] M. Cleary, M. Hodes, R. Grimes, and M. T. North, "Characterisation of a variable conductance heat pipe prototype for a photonic application," presented at the Proc. ASME, Vancouver, BC, Canada, Jul. 8–12, 2007.
- [18] L. W. da Silva and M. Kaviany, "Micro-thermoelectric cooler: Interfacial effects on thermal and electrical transport," *Int. J. Heat Mass Transfer*, vol. 47, pp. 2417–2435, 2004.



**Anthony M. Pettes** received the B.S.E. degree in mechanical engineering and B.A. in geology from Duke University, Durham, NC, in 2001 and the M.S. degree in mechanical engineering from Stanford University, Stanford, CA, in 2007.

His area of interest is heat transfer in micro-electronic devices. Current efforts are focused on thermoelectric device optimization in the presence of thermal and electrical boundary resistances.

Mr. Pettes is funded by the Bell Labs Graduate Research Fellowship Program, NASA Harriet G. Jenkins Pre-Doctoral Fellowship Program, and the National Science Foundation Graduate Research Fellowship Program.



**Marc S. Hodes** received the B.S. degree in mechanical engineering (with highest honors) from the University of Pittsburgh, Pittsburgh, PA, the M.S. degree in mechanical engineering from the University of Minnesota, Minneapolis, and the Ph.D. degree in mechanical engineering from the Massachusetts Institute of Technology, Cambridge, in 1998. The experimental portion of the Ph.D. degree was performed at the National Institute of Standards and Technology (NIST) in the capacity of a Guest Researcher and NSF/NIST Fellow.

He was a Member of the Technical Staff at Bell Laboratories, Murray Hill, NJ. He is now with Bell Labs Ireland, Alcatel-Lucent, Dublin, Ireland. His area of interest is heat transfer. Current efforts are focused on the thermal management of electronics and projects include those on increased-efficiency thermoelectric conversion, enhanced microchannel cooling using superhydrophobic, nanostructured surfaces, and mechanical alternatives to elastomeric gap fillers.



**Kenneth E. Goodson** received the S.B. degrees in mechanical engineering and humanities in 1989 and the M.S. and Ph.D. degrees in mechanical engineering from the Massachusetts Institute of Technology, Cambridge, in 1991 and 1993, respectively.

After graduation, he spent 18 months with the materials group at DaimlerBenz AG working on diamond heat sinks. He joined the Mechanical Engineering Faculty at Stanford University, Stanford, CA, in 1994, and his research group is a leader in the area of electronics cooling. He cofounded Cooligy in 2001 during a leave of absence from Stanford University, and the startup develops and supplies pumped liquid cooling systems for computers. From a fundamental perspective, his group studies heat transfer at very small length and time scales, in particular those relevant to the design of transistors, semiconductor lasers, and microelectromechanical systems (MEMS). His students have contributed to the development of two-phase microchannel and micro-jet impingement cooling technology for semiconductor chips. He has authored or coauthored more than 150 journal and conference papers and five book chapters.

Prof. Goodson has received a number of awards in recognition of his work, including the ONR Young Investigator Award, the NSF CAREER Award, the Journal of Heat Transfer Outstanding Reviewer Award (1999), a JSPS Visiting Professorship at the Tokyo Institute of Technology (1996), as well as Best Paper Awards at SEMI-THERM (2001), the Multilevel Interconnect Symposium (1998), and SRC TECHCON (1998).